

Synthesis, ^1H and ^{13}C NMR assignment and electrochemical properties of novel thiophene–thiazolothiazole oligomers and polymers

S. Van Mierloo,^a S. Chambon,^a A. E. Boyukbayram,^{a,b} P. Adriaensens,^a L. Lutsen,^c T. J. Cleij^a and D. Vanderzande^{a*}

Novel hexyl-substituted bithiophene compounds containing a thiazolothiazole(5,4-*d*) unit have been explored. The molecules are soluble in common organic solvents, which would enhance their chance of possible integration in printable electronics. Synthesis and complete elucidation of the chemical structures by detailed 1D/2D NMR spectroscopy are described. This provides interesting input for chemical shift prediction software, because few experimental data on this type of compounds are available. Furthermore, the potential n-type character of these derivatives is verified using electrochemical measurements. In addition, the low-bandgap character of conjugated polymers containing the thiazolothiazole unit is demonstrated by performing an electropolymerization. Copyright © 2010 John Wiley & Sons, Ltd.

Keywords: NMR; ^1H ; ^{13}C ; thiazolothiazole derivatives; chemical shift; prediction software; electropolymerization

Introduction

Organic field-effect transistors (OFETs)^[1] based on organic semiconductors attract considerable attention for applications such as flexible displays, low-cost electronic paper and smart memory/sensor elements. There are many low molecular weight hole-transporting (p-type) semiconductors, such as pentacene^[2] and oligothiophenes.^[3] However, the number of n-type organic semiconductors is still limited and the FET performances are not satisfactory. In the literature, a series of small n-type bithiophenes bearing a thiazolothiazole unit have been reported, which have high charge carrier mobilities.^[4] The thiazolothiazole unit has some excellent characteristics for use in electronic applications. First of all, its electron-accepting property is useful to enhance the stability toward oxygen. Consequently, these compounds are stable in ambient atmospheres at room temperature over a period of several months.^[5] Secondly, the thiazolothiazole moiety has a rigid planar structure due to the fused ring system, which can lead to efficient intermolecular $\pi-\pi$ interactions.^[4,6,7] Finally, the 2,5-bis-substituted thiazolothiazole is quite straightforward to prepare, starting from the corresponding aldehyde and dithioamide. The interesting parent compound thiazolothiazole(5,4-*d*) has already been synthesized many years ago in moderate yield, by combining an aldehyde derivative with dithioamide at very high temperature.^[8,9] Unfortunately, non-alkylsubstituted derivatives are very poorly soluble and require vacuum deposition techniques for device fabrication. Here, alternatively, a series of analogous thiazolothiazole containing molecules are presented, which do not have the above-mentioned disadvantages. To this end, the synthesized molecules, i.e. **D1**, **D2** and **D3** (cf Fig. 1) have been functionalized with two substituted 3-hexylthiophenes. The choice of substitution with alkyl chains leads to a significantly improved

solubility in common organic solvents. Hence, functionalization, purification and characterization become more straightforward and the molecules can be utilized in solvent-based processing, such as printable electronics. Moreover, the alkyl chains might improve stacking properties and, consequently, positively impact the charge mobilities in OFETs.

In this paper, we report the synthesis, detailed NMR structural elucidation and electrochemical properties of the first series of novel alkylthiophenylsubstituted thiazolothiazole oligomers. Cyclic voltammetry (CV) was used to verify the potential n-type character of these compounds and to estimate their highest occupied molecular orbital (HOMO) and lowest unoccupied molecular orbital (LUMO) energy levels. In addition, the molecules were used as monomers in an electropolymerization to demonstrate the low-bandgap character of conjugated polymers containing thiazolothiazole units.

* Correspondence to: D. Vanderzande, Hasselt University, Institute for Materials Research (IMO), Universitaire Campus, Building D, B-3590 Diepenbeek, Belgium. E-mail: dirk.vanderzande@uhasselt.be

a Hasselt University, Institute for Materials Research (IMO), Universitaire Campus, Building D, B-3590 Diepenbeek, Belgium

b Department of Chemistry, Karabuk University, 78050 Karabuk, Turkey

c IMEC, Division IMOMEC, Universitaire Campus, Wetenschapspark 1, B-3590 Diepenbeek, Belgium

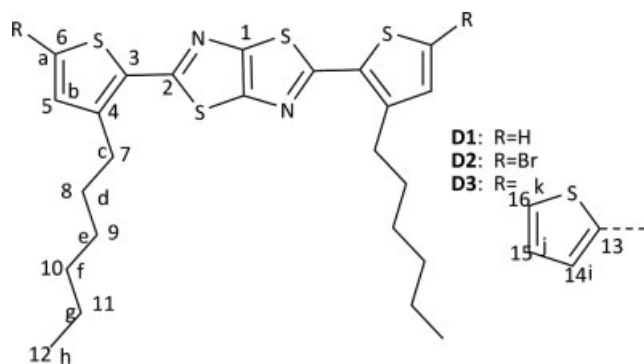
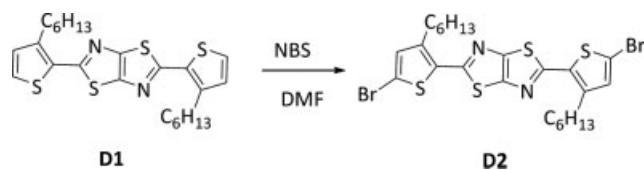


Figure 1. Chemical structures of the 2,5-bis(3-hexylthiophen-2-yl)thiazolo [5,4-*d*] thiazole derivatives **D1**, **D2** and **D3**. The different carbon atoms are numbered from C1 to C16 and the different hydrogen atoms are labeled from H-a to H-k.



Scheme 1. Synthetic route toward **D2**.

Results and Discussion

Synthesis

The first molecule, i.e. 2,5-bis(3-hexylthiophene-2-yl)thiazolo(5,4-*d*)thiazole **D1**, was synthesized via a condensation reaction between 3-hexylthiophene-2-carbaldehyde and dithiooxamide. 3-Hexylthiophene-2-carbaldehyde was prepared according to a modified literature procedure.^[5,10] Instead of iodine-activated magnesium turnings, *n*-butyllithium was used to create an anion at the 2-thiophenyl position, followed by a nucleophilic addition on DMF resulting in 3-hexylthiophene-2-carbaldehyde. The resulting compound **D1** was purified by column chromatography and two consecutive recrystallizations from ethanol and acetonitrile. **D1** was obtained as yellow crystals in 47% yield. In order to functionalize compound **D1**, a bromination reaction with NBS was carried out in DMF, giving 2,5-bis(5-bromo-3-hexylthiophene-2-yl)thiazolo(5,4-*d*)thiazole **D2** in 71% yield (Scheme 1).

Functionalization of **D2** was readily achieved by using a Stille cross coupling with tributyl(thiophen-2-yl)stannane under catalytic conditions with Pd(PPh₃)₄ resulting in 2,5-bis(4-hexyl-2,2'-bithiophene-5-yl)thiazolo(5,4-*d*)thiazole **D3** (Scheme 2). This product was also purified by column chromatography followed by recrystallization from ethanol resulting in **D3** in 58% yield. The purity of **D1** and **D3** was further confirmed by HPLC as being higher than 99%.

Due to the substitution with hexyl side chains, all three compounds **D1**, **D2** and **D3** are soluble in common organic solvents such as chloroform, dichloromethane and ethers. To confirm the identity of the synthesized structures, complete NMR characterization was performed. To this end, in the following section, the complete structural elucidation of the three synthesized compounds **D1**, **D2** and **D3** will be presented.

NMR characterization

In order to confirm the structure of the three thiazolothiazole derivatives (**D1**, **D2** and **D3**), they were studied extensively by NMR in order to perform a complete assignment of their ¹³C and ¹H resonances. Table 1 presents an overview of all signal assignments. Such a detailed analysis is advantageous, because the obtained chemical shift information can be very useful for implementation in NMR-based prediction software. The chemical structures of all the three compounds differ only at the 5-position of the thiophene rings: **D1** bears two hydrogen atoms, **D2** two bromine atoms and **D3** two unsubstituted thiophene rings. Figure 1 shows the structures of **D1**, **D2** and **D3**, together with an arbitrary numbering given to their different carbons and hydrogens. APT, DEPT, *T*₁*C* and short-range/long-range HETCOR experiments were performed on these compounds in order to obtain a complete chemical shift assignment of the ¹³C and ¹H resonances.

Assignment of the resonances of the core of **D1** and **D2**

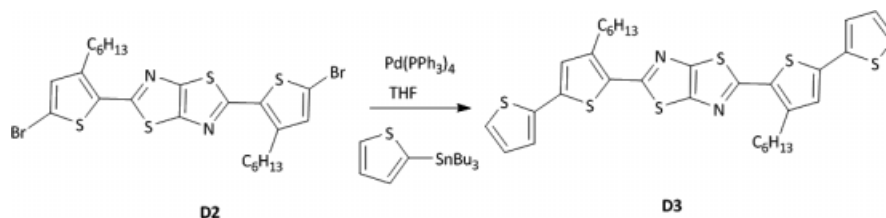
APT, DEPT and short-range HETCOR. The core of the derivatives is formed by six different carbons, C1 to C6. For **D2**, it appears that the 160.9, 150.7, 144.0, 134.0 and 116.1 ppm signals are quaternary carbons and only the 134.1 ppm signal is a methine carbon. The latter, therefore, corresponds to C5. The short-range HETCOR experiment indicates that the 134.1 ppm carbon signal is connected (¹*J* or direct coupling) to a proton singlet resonance at 6.93, corresponding to H-b.

In **D1**, the 162.2, 150.7, 143.8 and 132.5 ppm signals arise from non-protonated carbons, whereas the 131.5 and 128.0 ppm signals arise from CH-carbons. The short-range HETCOR indicates that the 131.5 ppm signal is attached to a ¹H doublet at 6.96/6.98 ppm and the 128 ppm signal to another ¹H doublet at 7.32/7.34 ppm. Based on the results obtained for **D2**, the ¹H doublet at 6.96/6.98 ppm can be legitimately attributed to H-b and the 131.5 ppm ¹³C resonance to C5. By deduction, the 128 ppm resonance can then be attributed to C6 and the ¹H doublet at 7.32/7.34 ppm to H-a. Moreover, this assignment is confirmed by the resonance frequency of H-a. Indeed the neighboring sulfur atom has a deshielding effect on the proton H-a, leading to a resonance signal at lower field as compared with H-b.

Long-range HETCOR. For both derivatives **D1** and **D2**, the signals at 162.2 and 150.7 ppm/160.9 and 150.7 ppm show no coupling with protons. Those signals therefore can be attributed to C2 and C1 (Table 1; *vide infra*) because both of them are at least four bonds away from a hydrogen atom.^[11]

In **D1**, the remaining carbon signals (143.8 and 132.5 ppm) should therefore correspond to C3 and C4. The long-range HETCOR experiment shows that the 132.5 ppm signal correlates only with the 6.96/6.98 ppm ¹H doublet, whereas the 143.8 ppm resonance is coupled to both the 7.32/7.34 ppm ¹H doublet (H-a) and the triplet centered at 2.86 ppm, corresponding to H-c. The fact that the 143.8 ppm signal is coupled with H-a indicates that it corresponds to C4. Indeed, C3 is too far (four bonds) from H-a to have a coupling with it. Hence, by deduction the 132.5 ppm signal corresponds to C3.

In **D2**, three quaternary carbon signals have a long-range coupling (²*J* or ³*J*) with protons, i.e. 116.1 ppm with H-b, 134.0 ppm with H-b and 144.0 ppm with H-a and H-c. The latter cannot correspond to C6 as it is four bonds away from H-c. By comparison with its hydrogenated equivalent (**D1**), it is possible to attribute

Scheme 2. Synthetic route toward **D3**.**Table 1.** Chemical shifts (ppm) and assignments of the proton and the carbon atoms in the thiazolothiazole derivatives **D1–D3**. The chemical shift scales are calibrated to TMS at 0 ppm

Atom	D1 R = H	D2 R = Br	D3 R = thiophen-2-yl	D1 R = H	D2 R = Br	D3 R = thiophen-2-yl
Carbon				Protons		
C1	150.7	150.7	150.7	–	–	–
C2	162.2	160.9	161.5	–	–	–
C3	132.5	134.0	131.0	–	–	–
C4	143.8	144.0	144.5	–	–	–
C5	131.5	134.1	127.6	H-b	6.97 (d)	6.93 (s)
C6	128.0	116.1	137.3	H-a	7.33 (d)	–
C7	30.8	30.9	31.1	H-c	2.95 (t)	2.84 (t)
C8	30.7	30.4	30.5	H-d	1.7 (q)	1.66 (q)
C9	30.0	30.0	30.1	H-e	1.42 (q)	1.42 (q)
C10	32.3	32.3	32.3	H-f	1.3 (m)	1.32 (m)
C11	23.3	23.3	23.3	H-g	1.3 (m)	1.32 (m)
C12	14.8	14.8	14.8	H-h	0.88 (t)	0.89 (t)
C13	–	–	139.4	–	–	–
C14	–	–	125.2	H-i	–	–
C15	–	–	128.8	H-j	–	–
C16	–	–	126.0	H-k	–	–

144.0 ppm to C4 and 134.0 ppm to C3. By elimination, C6 in the brominated sample has a resonance signal at 116.1 ppm.

Concerning the two remaining carbon signals of the core of **D1**, one can observe that the resonance at 162.2 ppm shifts to 160.9 when the thiazolothiazole compound is brominated. However, the other signal at 150.7 ppm remains unchanged. The latter can be attributed to C1 as it is the carbon most remote from the substituent on C6. Most conclusions can be confirmed by ^{13}C spin-lattice relaxation time (T_{1C}) experiments (Table 2). Carbon nuclei mainly relax through space via the surrounding magnetic moments of protons ($1/T_{1C}$ has a $1/r^6$ dependency). These proton magnetic moments induce local oscillating magnetic fields due to molecular motions; the source of T_1 relaxation.^[12] As the 150.7 ppm signal has the longest relaxation time, its corresponding carbon atoms indeed should be the most remote from protons. C2, being spatially more close to protons (e.g. H-c), therefore corresponds to the resonance signal at 162.2 in **D1** and 160.9 in **D2**. In addition, the assignment of C3 and C4 in **D1** can be confirmed by means of the T_{1C} relaxation decay times, being clearly longer (less efficient relaxation) for C3. The same holds true for **D2** sharing a decrease in the T_{1C} in going from C3 over C6 to C4.

Assignment of the resonances of the core of **D3**

The ^1H spectrum presents four resonance patterns corresponding to the four protons of the core: a singlet at 7.00 ppm and three double doublets at 7.02 ppm ($^3J = 3.7$ Hz, $^3J = 5.1$ Hz), 7.22 ppm

Table 2. ^{13}C spin-lattice relaxation decay times (T_{1C}) for all carbon signals of **D1** and **D3**

D1		D3	
^{13}C resonance frequency (ppm)	T_{1C} (s)	^{13}C resonance frequency (ppm)	T_{1C} (s)
162.2	14.2	161.5	6.7
150.7	21.1	150.7	9.3
143.8	6.6	144.5	3.3
132.5	15.9	139.4	4.0
131.5	0.66	137.3	6.1
128	0.72	131.0	7.8
32.3	2.01	128.8	0.63
30.8	0.74	127.6	0.40
30.7	1	126.05	0.41
30.0	1.3	125.2	0.63
23.3	2.9	32.3	1.67
14.8	3.2	31.1	0.50
		30.5	0.71
		30.1	1.00
		23.3	2.32
		14.8	3.12

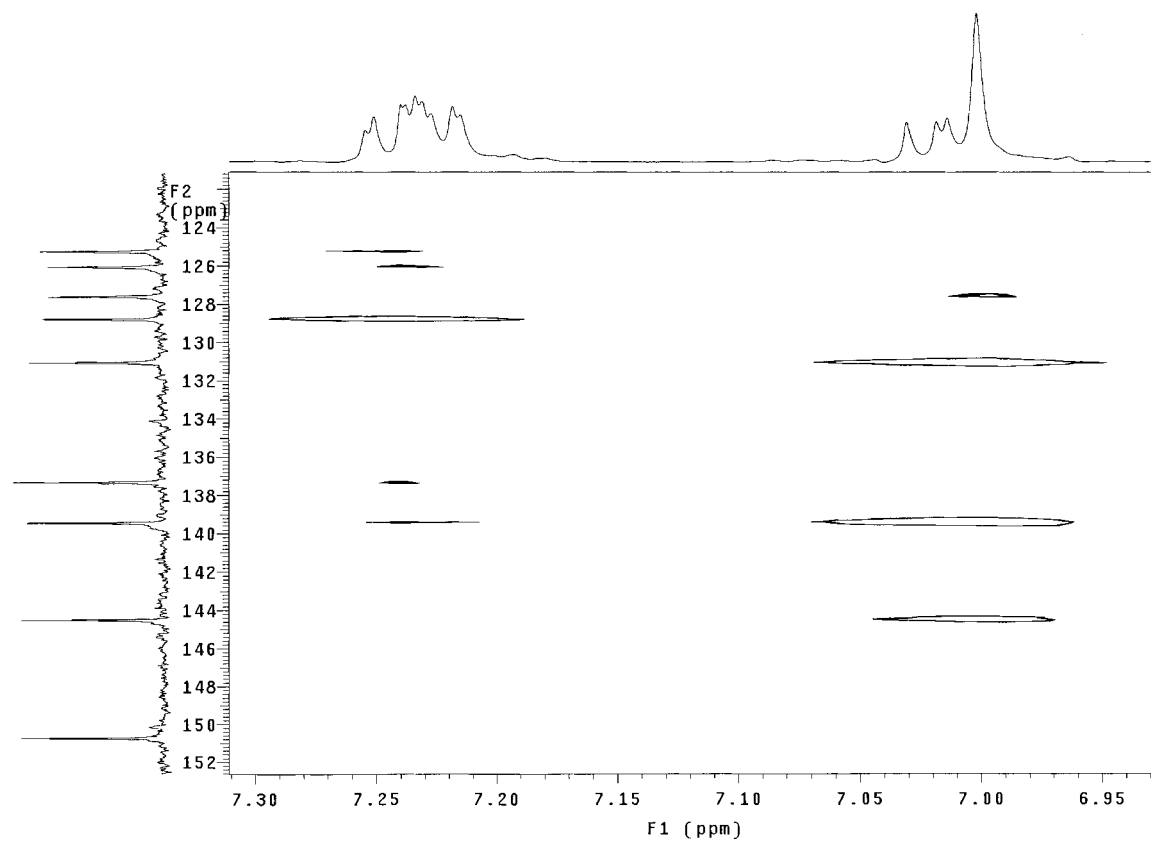


Figure 2. Long-range HETCOR ($J = 8$ Hz) of D3.

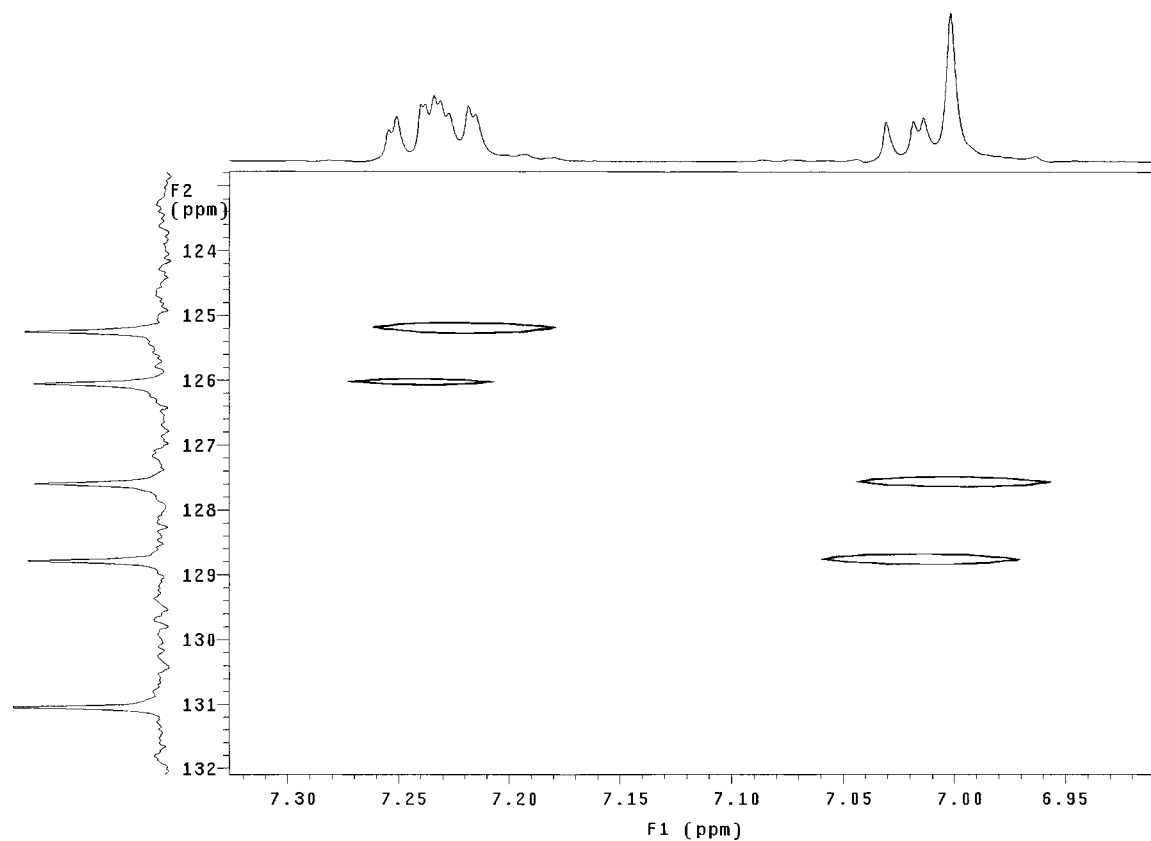


Figure 3. Short-range HETCOR ($J = 140$ Hz) of D3.

($^3J = 3.7$ Hz, $^4J = 1.0$ Hz) and 7.24 ppm ($^3J = 5.1$ Hz, $^4J = 1.0$ Hz). According to the J -coupling pattern and the literature data,^[12] these four signals correspond to H-b, H-j, H-i and H-k, respectively.

Concerning the assignment of the carbons, the assignments for **D1** and **D2** already allow the assignment of the core carbon signals at 161.5, 150.7, 144.5 and 131.0 ppm to C2, C1, C4 and C3, respectively. From the remaining six carbons of the core, the ones resonating at 137.3 and 139.4 ppm are quaternary carbons and correspond to C6 and C13. The long-range HETCOR experiment (Fig. 2) showed that the 139.4 ppm signal couples with H-b, H-i and H-j, whereas the 137.3 ppm signal has only a small coupling with H-i. This allows to assign the 139.4 ppm signal to C13 as C6 is separated by four bonds from H-j. C6 then corresponds to the signal at 137.3 ppm. This attribution is further confirmed by the T_{1C} relaxation which shows a longer decay time for the 137.3 ppm signal as compared with the 139.4 ppm one (6.1 and 4 s, respectively).

According to the short-range HETCOR (Fig. 3), the four remaining signals at 128.8, 126.0, 125.2 and 127.6 ppm are respectively coupled with the double doublets centered at 7.02 (H-j), 7.24 (H-k), 7.22 (H-i) and the singlet at 7.00 (H-b) ppm. They correspond to C15, C16, C14 and C5, respectively.^[13]

Alkyl side chain resonance assignment

The attribution of the carbon and proton signals is only described for **D1** as the same procedure holds for **D2** and **D3**.

The chemical shift and J -coupling pattern of the 2.95 and 0.88 ppm signals indicate that they correspond to H-c and H-h, respectively. The short-range HETCOR experiment already attributed their corresponding carbon signals to 30.8 and 14.8 ppm, respectively.

In order to assign the four remaining side chain carbon signals and their respective protons, ^{13}C spin-lattice relaxation time (T_{1C}) and COSY experiments were performed. Table 2 summarizes the T_{1C} values for the different carbon signals. For mobile side chains, the closer the carbon is situated toward the side chain end, the longer its relaxation decay time will be due to less restricted conformational motions.^[12] This is clear for C7 (30.8 ppm) and C12 (14.8 ppm) which have respectively the shortest and the longest T_{1C} time constant of the alkyl chain carbons. Following this theory, we can attribute the 30.7, 30.0, 32.3 and 23.3 ppm signals to C8, C9, C10 and C11, respectively. The short-range HETCOR spectrum allows the assignment of their respective proton signals and the COSY experiment confirmed these attributions.

Electrochemical characterization

As NMR has confirmed that compounds **D1** and **D3** were available in excellent purity, the electrochemical properties, which are important toward potential application, can now be investigated. CV was employed to investigate the electrochemical behavior of **D1** and **D3** and to estimate their HOMO and LUMO energy levels. In addition, the compounds were electropolymerized under the same conditions. Upon electropolymerization, a dark red polymer was obtained with **D1** as monomer and a grayish-blue polymer was obtained with **D3** as monomer. The intensity of the color and the film thickness increased with polymerization time. However, after 1 h of polymerization, no further increase in the thickness was observed. In addition, for both monomers, no bulk polymer was observed in solution. For the CV of the polymers, the formed polymer films were first rinsed with CH_3CN , after which a fresh electrolyte solution was added.

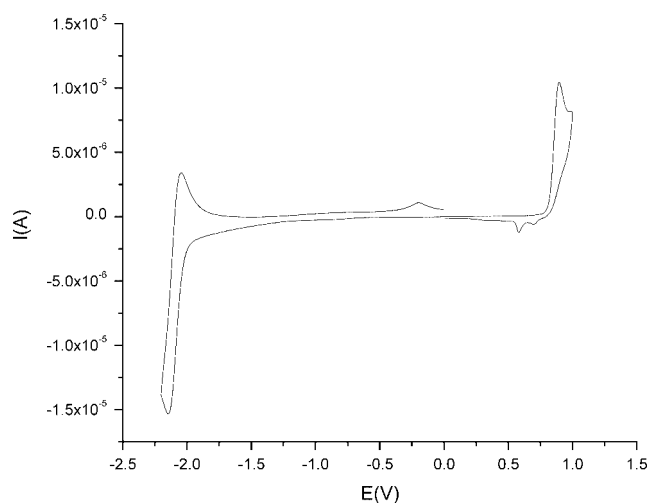


Figure 4. Cyclic voltammograms of **D1** (solid: 1st scan; dashed: 2nd scan; dotted: 3rd scan).

Table 3. HOMO–LUMO and optical/electrochemical energy gap values of **D1** and **D3** as well as the corresponding electropolymerized conjugated polymers **P1** and **P3**

	HOMO (eV)	LUMO (eV)	E_g^{EC} (eV)	E_g^{OP} (eV) ^a (solution)	E_g^{OP} (eV) ^a (thin film)
D1	−5.74	−2.91	2.83	2.84	
P1	−5.26	−3.43	1.83		1.9
D3	−5.54	−3.14	2.40	2.46	
P3	−5.25	−3.51	1.74		1.7

^a Determined by means of UV–Vis spectroscopy.

The cyclic voltammogram of monomer **D1** displays typical oxidation and reduction processes as shown in Fig. 4. The HOMO–LUMO gap was calculated at 2.83 eV using the onset values of oxidation and reduction and corresponding HOMO–LUMO values (Table 3). The sharp oxidation peak around 0.670 V in Fig. 4, which occurs after the first scan, is a result of the formation of an intermediate oligomer. Upon further electropolymerizing of **D1** (Fig. 5), the oxidation peak of the conjugated polymer (**P1**, *cf* Fig. 6) appears at *ca* 0.5 V. The final onset values of the oxidation and reduction of **P1** are 0.325 and −1.505 V, from which the electrochemical energy gap can be estimated at 1.83 eV (Table 3). The LUMO of **P1** can be readily determined at −3.43 eV (Table 3), which is more accurate than a previously reported value, which was indirectly obtained from the oxidation potential and the optical bandgap.^[5]

The onset values of the oxidation and reduction for **D3** give an electrochemical HOMO–LUMO gap of 2.40 eV (Fig. 7). After several scans, the oxidation peak of the corresponding conjugated polymer (**P3**, *cf* Fig. 6) appears around 0.6 V (Fig. 8). The final onset values of the oxidation and reduction of **P3** are 0.315 and −1.425 V, from which the electrochemical energy gap can be estimated at 1.74 eV (Table 3).

It is noteworthy that both **D1** and **D3** exhibit a distinct reversible reduction peak in their cyclic voltammograms. This confirms the potential n-type character of these compounds. However, a more thorough mobility study has to be performed to confirm the n-type character. Furthermore, the HOMO–LUMO energy gap

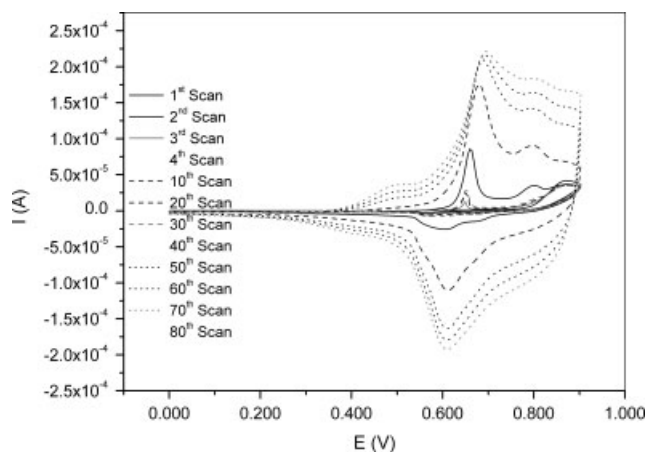


Figure 5. Electropolymerization of **D1**. Every 10th of 80 consecutive scans is presented.

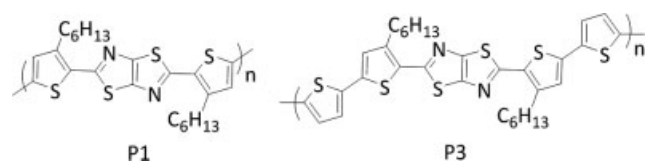


Figure 6. Chemical structures of polymers **P1** and **P3**.

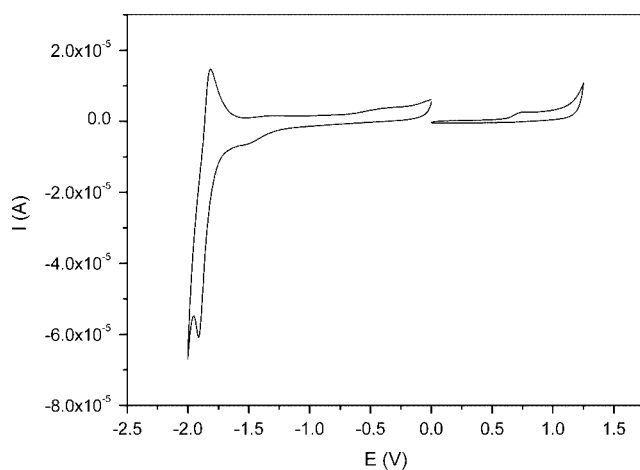


Figure 7. Cyclic voltammogram of **D3**.

values of both monomers and polymers are in good agreement with their corresponding optical energy gaps (Table 3). In addition, the low-bandgap character of conjugated polymers containing thiazolothiazole units is demonstrated by the electrochemical energy gap values observed for **P1** and **P3**, which are both below 2 eV.

Conclusion

Substitution of thiophene-thiazolothiazole derivatives **D1**, **D2** and **D3** with hexyl side chains noticeably improved their solubility in common organic solvents. As a result, **D1** and **D2** could readily undergo functionalization reactions to become suitable for printable electronics. The proposed chemical structures of **D1**–**D3**

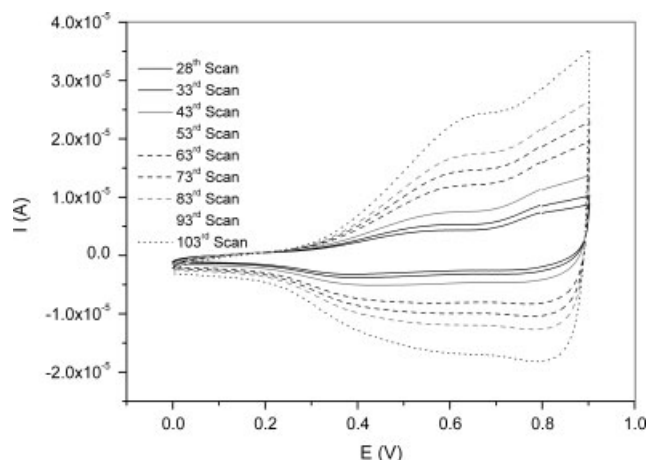


Figure 8. Electropolymerization of **D3**. Selective scans of a total of 103 consecutive scans are presented.

are fully confirmed by NMR spectroscopy. A complete assignment of the proton and carbon resonances was accomplished by means of 1D- and 2D-NMR experiments. As it concerns rather newly developed compounds, such a complete signal assignment will be highly useful for further progression in NMR prediction software. CV was used to estimate the HOMO and LUMO energy levels of **D1** and **D3**. These values, in combination with the reversible character of the reduction processes, indicate that these compounds potentially have an n-type character. In addition, **D1** and **D3** were used as monomers in an electropolymerization and it was demonstrated that the conjugated polymers containing the thiophene-thiazolothiazole core as building block can have a low-bandgap character.

Experimental

Synthesis

Tributyl(thiophen-2-yl)stannane was synthesized according to the literature procedure.^[14]

3-Hexylthiophene-2-carbaldehyde

A solution of 2-bromo-3-hexylthiophene (5.7 g, 0.023 mol) in THF (150 ml) was cooled down to -78°C , after which *n*-butyllithium (14 ml, 0.023 mol, 1.6 M in hexane) was slowly added under N_2 atmosphere. After the mixture was stirred for 15 min, dry DMF (2.40 ml, 0.031 mol) was added dropwise at the same temperature. Subsequently, the mixture was warmed up to room temperature and stirred for an additional 2 h. Afterward the reaction mixture was treated with a HCl-solution (0.5 M) and extracted with diethyl ether (3×50 ml). The combined organic layers were washed with saturated bicarbonate solution and brine, dried over magnesium sulfate and concentrated by evaporation *in vacuo*. The crude product was purified by column chromatography using silica gel (eluent: hexane/ethylacetate 95 : 5) giving 3.20 g of a viscous yellow oil (71% yield).

$^1\text{H NMR}$ (CDCl_3): $\delta = 9.95$ (s, 1H), 7.55 (d, $J = 5.1$ Hz, 1H), 6.93 (d, $J = 5.1$ Hz, 1H), 2.88 (t, 2H), 1.58 (m, 2H), 1.21 (m, 6H), 0.80 (t, 3H).

2,5-Bis(3-hexylthiophene-2-yl)thiazolo(5,4-d)thiazole **D1**

A mixture of 3-hexylthiophene-2-carbaldehyde (3.02 g, 0.015 mol) and dithioamide (0.29 g, 2.42 mmol) was stirred at 200°C for

2 h. Subsequently, the reaction mixture was cooled down to room temperature and diluted with water (50 ml) and diethyl ether (50 ml). The organic layer was separated and the aqueous layer was extracted with diethyl ether (3 × 50 ml). The combined organic layers were washed with a saturated bicarbonate solution and brine, dried over magnesium sulfate and concentrated by evaporation *in vacuo*. The resulting brown oil was purified by column chromatography using silica gel (eluent: hexane/ethyl acetate 95:5) followed by subsequent recrystallization from acetonitrile and ethanol giving 0.54 g of yellow crystals (47% yield).

$^1\text{H NMR}$ (CDCl_3): $\delta = 7.33$ (d, $J = 5.1$ Hz, 2H), 6.97 (d, $J = 5.1$ Hz, 2H), 2.95 (t, 4H), 1.7 (q, 4H), 1.42 (q, 4H), 1.3 (m, 4H), 1.3 (m, 4H), 0.88 (t, 6H); MS: $m/z = 474$ (M^+); UV-Vis (solution chloroform) (λ_{max}) 392 nm, m.p. = 71 °C.

2,5-Bis(5-bromo-3-hexylthiophene-2-yl)thiazolo(5,4-d)thiazole D2

Protected from light, a solution of NBS (0.61 g, 3.44 mmol) in DMF (50 ml) was added dropwise to a solution of 2,5-bis(3-hexylthiophene-2-yl)thiazolo(5,4-d)thiazole **D1** (0.51 g, 1.08 mmol) in DMF (50 ml), after which the mixture was stirred for 48 h. Subsequently, the mixture was poured onto ice and extracted with diethyl ether (3 × 50 ml). The combined organic layers were washed with a saturated bicarbonate solution and brine, dried over magnesium sulfate and concentrated by evaporation *in vacuo*. The crude solid was purified by column chromatography using silica gel (eluent: hexane/ethyl acetate 95:5). The compound was obtained as an orange solid (0.48 g, 71% yield).

$^1\text{H NMR}$ (CDCl_3): $\delta = 6.93$ (s, 2H), 2.84 (t, 4H), 1.66 (q, 4H), 1.42 (q, 4H), 1.32 (m, 4H), 1.32 (m, 4H), 0.89 (t, 6H); MS: $m/z = 632$ (M^+); UV-Vis (solution chloroform) (λ_{max}) 393 nm.

2,5-Bis(4-hexyl-2,2'-bithiophene-5-yl)thiazolo(5,4-d)thiazole D3

A solution of tributyl(thiophen-2-yl)stannane (0.47 g, 1.26 mmol) in dry THF (50 ml) was added dropwise to a stirred mixture of 2,5-bis(5-bromo-3-hexylthiophene-2-yl)thiazolo(5,4-d)thiazole **D2** (0.32 g, 0.51 mmol) and $\text{Pd}(\text{PPh}_3)_4$ (0.003 g, 2.60 μmol) in dry THF (50 ml) at ambient temperature. After stirring for 12 h at reflux temperature, the reaction mixture was diluted with water (50 ml). The organic layer was separated and the aqueous layer was extracted with diethyl ether (3 × 50 ml). The combined organic layers were washed with a saturated bicarbonate solution and brine, dried over magnesium sulfate and concentrated by evaporation *in vacuo*. The reaction product was purified by column chromatography (eluent: hexane/ethyl acetate 95:5) and recrystallized from ethanol resulting in 0.19 g of red crystals (58% yield).

$^1\text{H NMR}$ (CDCl_3): $\delta = 7.24$ (dd, $J = 5.1$ Hz, $J = 1.0$ Hz, 1H), 7.22 (dd, $J = 3.7$ Hz, $J = 1.0$ Hz, 1H), 7.02 (dd, $J = 5.1$ Hz, $J = 3.7$ Hz, 1H), 7.00 (s, 2H), 2.88 (t, 4H), 1.71 (q, 4H), 1.45 (q, 4H), 1.34 (m, 4H), 1.34 (m, 4H), 0.90 (t, 6H); MS: $m/z = 638$ (M^+); UV-Vis (solution chloroform) (λ_{max}) 449 nm; m.p. = 153 °C.

Electrochemical characterization/electropolymerisation

Electrochemical measurements were performed with an Eco Chemie Autolab PGSTAT 30 Potentiostat/Galvanostat using 0.1 M Bu_4NPF_6 in anhydrous CH_3CN as the electrolyte under N_2 atmosphere. A three-electrode microcell was utilized containing

an Ag/AgNO₃ reference electrode (0.1 M AgNO₃ and 0.1 M Bu_4NPF_6 in CH_3CN), a platinum counter electrode and an indium tin oxide (ITO)-coated glass substrate as the working electrode. The respective monomers were dissolved to their maximum solubility in the electrolyte solution. Cyclic voltammograms were recorded at a scan rate of 50 mV/s. Oxidative electropolymerization was achieved by scanning between 0 and 0.9 V at the same scan rate for a large number of consecutive scans. For the conversion to electron volts, all electrochemical potentials have been referenced to a known standard (ferrocene/ferrocenium in CH_3CN , 0.05 V vs Ag/AgNO₃), which in acetonitrile solution is estimated to have an oxidation potential of -4.98 V *versus* vacuum. UV-Vis spectra were recorded on a Varian CARY 500 UV-Vis-NIR spectrophotometer from 200 to 800 nm at a scan rate of 600 nm/min.

NMR characterization

All ^1H and ^{13}C liquid-state NMR experiments on **D1**, **D2** and **D3** were performed at room temperature on a Varian Inova 300 spectrometer in a 5-mm four-nucleus PFG probe. Solutions were prepared in CDCl_3 with concentrations of 3 and 50 mg/ml for the ^1H and ^{13}C spectra, respectively. The chemical shift scales are calibrated to TMS at 0 ppm. The proton spectra were acquired with a 90° pulse of 4.3 μs , a spectral width of 4500 Hz, an acquisition time of 3.5 s, a preparation delay of 8 s and 20 accumulations, processed with a linebroadening of 0.2 Hz and a data matrix of 65k. The carbon spectra were acquired with a 90° pulse of 12 μs , a spectral width of 8500 Hz, an acquisition time of 0.8 s, a preparation delay of 60 s and 2500 accumulations, processed with a linebroadening of 3 Hz and a data matrix of 32k.

Acknowledgements

We gratefully acknowledge the EU for the FP6-Marie Curie-RTN 'SolarNtype' (MRTN-CT-2006-035533), the IWT (Institute for the Promotion of Innovation by Science and Technology in Flanders) for the financial support via the SBO-project 060843 'PolySpec'. We also want to thank BELSPO in the frame of network IAP P6/27 and for a post-doc fellowship (A. E. B.). Furthermore, the support of the Fund for Scientific Research-Flanders (FWO projects G.0161.03N, G.0252.04N and G.0091.07N) is acknowledged.

References

- [1] H. Klauk, *Organic Electronics: Materials, Manufacturing and Applications*, Wiley: Weinheim, 2006.
- [2] (a) D. J. Gundlach, J. A. Nichols, L. Zhou, T. N. Jackson, *Appl. Phys. Lett.* **2002**, *80*, 2925; (b) H. Meng, M. Bendikov, G. Mitchell, R. Helgeson, F. Wudl, Z. Bao, T. Siegrist, C. Kloc, C. H. Chen, *Adv. Mater.* **2003**, *15*, 1090; (c) J. E. Anthony, *Chem. Rev.* **2006**, *106*, 5028.
- [3] M. Halik, H. Klauk, U. Zschieschang, G. Schmid, S. Ponomarenko, S. Kirchmeyer, W. Weber, *Adv. Mater.* **2003**, *15*, 917.
- [4] S. Ando, J.-i. Nishida, H. Tada, Y. Inoue, S. Tokito, Y. Yamashita, *J. Am. Chem. Soc.* **2005**, *127*, 5336.
- [5] Naraso, F. Wudl, *Macromolecules* **2008**, *41*, 3169.
- [6] S. Ando, J.-i. Nishida, Y. Inoue, S. Tokito, Y. Yamashita, *J. Mater. Chem.* **2004**, *14*, 1787.
- [7] S. Ando, D. Kumaki, J.-i. Nishida, H. Tada, Y. Inoue, S. Tokito, Y. Yamashita, *J. Mater. Chem.* **2007**, *17*, 553.
- [8] J. R. Johnson, R. Ketcham, *J. Am. Chem. Soc.* **1960**, *82*, 2719.
- [9] J. R. Johnson, D. H. Rotenberg, R. Ketcham, *J. Am. Chem. Soc.* **1970**, *92*, 4046.

- [10] I. Osaka, G. Sauvé, R. Zhang, T. Kowalewski, R. D. McCullough, *Adv. Mater.* **2007**, *19*, 4160.
- [11] A. Rössler, P. Boldt, *J. Chem. Soc., Perkin Trans.* **1998**, *1*, 685.
- [12] P. J. Adriaensens, F. G. Karssenbergh, J. M. Gelan, V. B. F. Mathot, *Polymer* **2003**, *44*, 3483.
- [13] E. Pretsch, P. Bühlmann, C. Affolter, *Structure Determination of Organic Compounds*, Springer-Verlag: New York, **2000**.
- [14] T. Pinault, F. Chérioux, B. Therrien, G. Süß-Fink, *Heteroatom Chem.* **15**, **2004**, 121.